

Nuclear scattering of low energy pions

K. Stricker, H. McManus, and J. A. Carr

Cyclotron Laboratory, Department of Physics and Astronomy, Michigan State University, East Lansing, Michigan 48824

(Received 1 May 1978)

We have estimated the parameters of the optical potential for low energy pion-nucleus scattering from the values obtained empirically in the analysis of pionic atom data. The ambiguities in these parameters are discussed. The shape of the low energy elastic scattering cross section for light elements is particularly sensitive to the relative strength of the repulsive and velocity-dependent attractive parts of the optical potential, and is well reproduced by pionic atom parameters. Absorption is the dominant reaction channel at low energies. Pion nucleon phase shifts are used to extrapolate optical model parameters to higher energies. The behavior of the elastic and inelastic angular distributions and of various partial cross sections is discussed, and compared with experiment.

NUCLEAR REACTIONS Calculated pion-nucleus optical potential, elastic scattering, inelastic scattering and partial cross sections. 30, 40, 50 MeV on various targets. 116-220 MeV on individual targets.

I. INTRODUCTION

Pion-nucleus scattering data have been appearing recently for pion kinetic energies of about 50 MeV, well below the (3, 3) resonance region. In the present work we first consider the optical potential developed to fit the shifts and widths of the energy levels in pionic atoms, and argue that the optical parameters are approximately constant over the energy range from 0 to 50 MeV. This suggests that these low energy scattering data should be reproduced by an optical potential only minimally different from that used for pionic atom analysis. We develop such an optical potential, and obtain reasonable fits to the elastic and inelastic data using pionic atom parameters. We also extrapolate the parameters to higher energy in order to compare the predicted difference between π^+ and π^- scattering with experiment.

II. PIONIC ATOM OPTICAL POTENTIAL

The optical potential for pionic atoms arises from a pion-nucleon scattering amplitude of the form

$$f = b_0 + b_1 \vec{t} \cdot \vec{\tau} + (c_0 + c_1 \vec{t} \cdot \vec{\tau}) \vec{k} \cdot \vec{k}', \quad (1)$$

neglecting a small spin dependent term. At very low energies the coefficients can be taken to be real. The finite widths of pionic atom levels indicate an imaginary part of the optical potential due to pion absorption. This is usually parametrized in terms of the square of the nuclear density, assuming absorption is due mainly to two-nucleon processes, i.e., *s*- and *p*-wave scattering from one nucleon followed by absorption on a neighboring nucleon. The optical potential $U_{opt}(r)$

can be written to first order in the multiple-scattering series,¹ with the addition of second order absorption terms, as

$$2\bar{\mu} U_{opt} = -4\pi(b(r) + p_2 B_0 \rho^2(r)) + 4\pi \vec{\nabla} \cdot \left(c(r) + \frac{C_0}{p_2} \rho^2(r) \right) \vec{\nabla}, \quad (2)$$

where

$$b(r) = p_1 (b_0 \rho(r) + b_1 [\delta \rho(r)])$$

and

$$c(r) = \frac{1}{p_1} (c_0 \rho(r) + c_1 [\delta \rho(r)]).$$

Here $\delta \rho(r) = \rho_n(r) - \rho_p(r)$, and $p_1 = 1 + \mu/M$ and $p_2 = 1 + \mu/2M$ are kinematic factors which arise from the transformation from the pion-nucleon center of mass (2CM) to the pion-nucleus center of mass (ACM) system. M is the nucleon mass, μ is the pion mass, and $\bar{\mu}$ is the reduced mass of the pion. Terms of order $1/A$ have been dropped. The matter density $\rho(r)$ is normalized such that $\int \rho(r) d\tau = A$. The neutron and proton densities are $\rho_n(r)$ and $\rho_p(r)$, normalized to N and Z respectively. The complex parameters B_0 and C_0 describe the absorption. The quantities b_0 , b_1 , c_0 , and c_1 obtained from the pion-nucleon scattering amplitudes will be referred to as the single nucleon parameters to distinguish them from the absorptive parameters. From the pion-nucleon phase shifts,² the isoscalar scattering length b_0 is found to be small but negative corresponding to a repulsive term in the optical potential arising from *s*-wave pion-nucleon scattering. The parameter c_0 is positive, corresponding to an attractive velocity-dependent potential arising from the *p*-wave

pion-nucleon scattering. Level shifts for light atoms do indeed show a repulsive potential for s states and an attractive potential for p states.

Ericson and Ericson³ showed that a potential of the form (2) is not sufficient to give reasonable fits to the pionic atom data; it is necessary to extend it to second order in the multiple-scattering series. This results in a potential of the form

$$2\bar{\omega}U_{\text{opt}} = -4\pi(b(r) + p_2 B_0 \rho^2(r)) + 4\pi\vec{\nabla} \cdot \left(L(r) \left[c(r) + \frac{C_0}{p_2} \rho^2(r) \right] \right) \vec{\nabla}, \quad (3)$$

where

$$b(r) = p_1(\bar{b}_0 \rho(r) + b_1[\delta\rho(r)]),$$

$c(r)$ is defined in Eq. (2),

and

$$L(r) = \left(1 + \frac{4\pi\lambda}{3} \left[c(r) + \frac{C_0}{p_2} \rho^2 \right] \right)^{-1},$$

This potential differs from the first order optical potential defined in (2) above in the following respects.

First, the parameter b_0 is replaced by \bar{b}_0 , the effective s -wave scattering length in a nucleus, where $\bar{b}_0 \approx b_0 - (3/2\pi)(b_0^2 + 2b_1^2)k_F$ and k_F is the Fermi momentum, taken to be 1.4 fm^{-1} . As b_0 is slightly repulsive but approximately zero owing to cancellation between $I = \frac{1}{2}$ and $I = \frac{3}{2}$ terms, this correction always increases the repulsion.

Second, the p -wave term is modified by the Ericson-Ericson factor, $L(r)$, which has the effect of weakening the p -wave attraction to an extent determined by the parameter λ . This factor arises from the inclusion of short range correlations between nucleons. The Ericson-Ericson factor has the effect of inhibiting second order scattering if the pion-nucleon p -wave interaction is of short enough range, as shown by Eisenberg, Hüfner, and Moins.⁴ If inhibition is complete, $\lambda = 1$, and the Born approximation is then, for a light nucleus, a good approximation to the scattering from this term of the optical potential (3).

III. ENERGY DEPENDENCE OF THE OPTICAL POTENTIAL PARAMETERS IN LOW ENERGY REGION

The single nucleon parameters b_1 , c_0 , and c_1 calculated from phase shifts² are quite constant over the energy range $T_\pi \lesssim 50 \text{ MeV}$. The parameter b_0 shows considerable scatter as a function

of energy, due to the near cancellation of the terms mentioned earlier. However, the s -wave phase shifts α_1 and α_3 , taken from the table in Ref. 2 labeled CERN theoretical, are approximately proportional to $k_{\text{c.m.}}$ for pion kinetic energies up to 50 MeV , yielding a value of b_0 which is constant in this energy range. The values estimated for the s -wave parameters are $b_0 \approx -0.020$ and $b_1 \approx -0.129$, giving $\bar{b}_0 \approx -0.042 \text{ fm}$. The p -wave parameters are $c_0 \approx 0.73 \text{ fm}^3$ and $c_1 \approx 0.44 \text{ fm}^3$.

The approximate constancy of the single nucleon parameters indicates the approximate constancy of the corresponding parameters of the optical potential itself over this energy range. Since the term in λ is due to short range correlations, the relevant parameter is (ka) with $a \approx 0.5 \text{ fm}$ and $k \approx 0.64 \text{ fm}^{-1}$ for $T_\pi = 50 \text{ MeV}$. This gives $ka \approx 0.32$ which is reasonably small; therefore λ might also be expected to vary slowly in this energy range. A detailed calculation, carried out originally by Thies⁵ and further refined by Brown, Jennings, and Rostokin,⁶ confirms the slow variation of these optical parameters in the low energy range. They show that effects due to short range nucleon-nucleon correlations, long range (Pauli) correlations, the strong interaction form factors, and the presence of the ρ meson in double scattering processes conspire to give a simple result. The absorption parameters $\text{Im}B_0$ and $\text{Im}C_0$ are functions of the single nucleon parameters, with slowly varying kinematical factors, so they too may be expected to vary little in this energy range. We conclude from this that the optical parameters for scattering of pions with $T_\pi \lesssim 50 \text{ MeV}$ should be almost the same as for pionic atoms, though there is little information, either theoretical or empirical, on the behavior of the dispersive parts $\text{Re}B_0$ and $\text{Re}C_0$.

IV. PION SCATTERING OPTICAL POTENTIAL

The wave equation we use to calculate the elastic scattering and to generate the distorted waves for inelastic scattering is of the form

$$(\nabla^2 + k^2 - 2\bar{\omega}U_{\text{opt}})\phi(r) = 0, \quad (4)$$

where k is the momentum of the pion in the ACM system, given by $k = k_L/(1 + \epsilon_0/A)$, and where $\bar{\omega}$ is the reduced energy given by $\bar{\omega} = \omega/(1 + \epsilon/A)$. Here we have defined k_L and ω_L as the momentum and total energy of the pion in the lab, and ω as the total energy of the pion in the ACM system. Also, $\epsilon_0 = \omega_L/M$ and $\epsilon = \omega/M$, where $M = (\text{nuclear mass})/A \approx 931 \text{ MeV}$. The complete optical potential used for pion scattering is of the form

$$\begin{aligned}
2\bar{\omega}U_{\text{opt}} = & -4\pi \left(b(r) + p_2 B_0 \rho^2(r) + \frac{(p_1 - 1)}{2} \nabla^2 c(r) \right. \\
& \left. + \frac{C_0(p_2 - 1)}{2p_2} \nabla^2 \rho^2(r) \right) \\
& + 4\pi \left(\vec{\nabla} \cdot L(r) c(r) \vec{\nabla} + \frac{C_0}{p_2} \vec{\nabla} \cdot \rho^2(r) \vec{\nabla} \right) + 2\bar{\omega} V_c(r),
\end{aligned} \tag{5}$$

where

$$\begin{aligned}
b(r) &= p_1 (\bar{b}_0 \rho(r) - \epsilon_\pi b_1 \delta \rho(r)), \\
c(r) &= \frac{1}{p_1} (c_0 \rho(r) - \epsilon_\pi c_1 \delta \rho(r)), \\
\delta \rho(r) &= \rho_n(r) - \rho_p(r),
\end{aligned}$$

and

$$L(r) = \left[1 + \frac{4\pi\lambda}{3} \left(\frac{A-1}{A} \right) c(r) \right]^{-1}.$$

The kinematical factors are

$$p_1 = \frac{1 + \epsilon}{1 + \epsilon/A}$$

and

$$p_2 = \frac{1 + \epsilon/2}{1 + \epsilon/A}.$$

The origin of these factors is discussed in the Appendix. In the limit of zero pion kinetic energy, p_1 and p_2 reduce to the form given for the pionic atom analysis when the terms in $1/A$ are dropped. The Coulomb potential is

$$V_c = \epsilon_\pi e^2 \int \frac{\rho_c(r')}{|r - r'|} d^3 r',$$

where $\epsilon_\pi = \pm 1$ gives the pion charge, and the charge distribution $\rho_c(r)$ is normalized such that $\int \rho_c(r) d\tau = Z$.

This potential is different in form from the pionic atom optical potential (3) in two important respects. First, the absorptive p -wave term is taken outside the Ericson-Ericson factor. The modifications to the argument in Ref. 3 due to the finite range of the interaction have not yet been explored, so we simply keep the leading term. Second, terms in $\nabla^2 \rho$ and $\nabla^2 \rho^2$ are included, following Thies.⁵ These terms arise from the transformation of the $\vec{k} \cdot \vec{k}'$ factor in the p -wave term from the 2CM system to the ACM system, often called the angle transformation.

The size parameters for the calculation were taken from the available tables.^{7,8} For low energy scattering, only a small momentum transfer range is covered, so $\rho_p(r)$ was obtained from $\rho_c(r)$ by adjusting only the size parameter of the distribution such that $R_c^2 = R_p^2 + 0.64$. This correction is

TABLE I. Geometrical parameters. Quantities with subscript c refer to charge densities; quantities without subscripts refer to matter densities.

${}^4\text{He}, {}^{12}\text{C}, {}^{16}\text{O}$:	$\rho \sim \left(1 + \alpha \frac{r^2}{a^2}\right) e^{-r^2/a^2}$	$\rho_c \sim \left(1 + \alpha \frac{r^2}{a_c^2}\right) e^{-r^2/a_c^2}$	
	a_c (fm)	a (fm)	α
${}^4\text{He}$	1.40	1.23	0
${}^{12}\text{C}$	1.66	1.57	1.33
${}^{16}\text{O}$	1.83	1.75	1.54
${}^{28}\text{Si}, {}^{40}\text{Ca}, {}^{90}\text{Zr}, {}^{208}\text{Pb}$:	$\rho \sim (1 + e^{(r-R)/a})^{-1}$	$\rho_c \sim \rho$	
	R (fm)	a (fm)	
${}^{28}\text{Si}$	2.93	0.569	
${}^{40}\text{Ca}$	3.51	0.563	
${}^{90}\text{Zr}$	4.83	0.496	
${}^{208}\text{Pb}$	6.46	0.542	

made for light nuclei up to ${}^{16}\text{O}$. The proton and neutron densities were taken to have the same geometry so that $\delta \rho(r)$ becomes $[(N - Z)/A] \rho(r)$. Parameters used in the calculations are given in Table I.

V. PARAMETERS OF THE OPTICAL POTENTIAL

Our intention is to calculate the pion-nucleus scattering cross section using the optical parameters which fit the pionic atom data. Lists of the parameters deduced from pionic atom analysis have been given by Hüfner in his review article.⁹ There exists no unique set of parameters as various analyses use slightly different forms for the optical potential. A thorough discussion is given in Refs. 9 and 10. A typical set of pionic atom empirical parameters is $\lambda \approx 1$ and

$$\bar{b}_0 = -0.042 \text{ fm } [-0.042 \text{ fm}],$$

$$b_1 = -0.11 \text{ fm } [-0.13 \text{ fm}],$$

$$c_0 = 0.63 \text{ fm}^3 [0.73 \text{ fm}^3], \quad c_1 = 0.60 \text{ fm}^3 [0.44 \text{ fm}^3],$$

$$B_0 = -0.17(1 - i) \text{ fm}^4, \quad C_0 = -0.53(1 - i) \text{ fm}^6,$$

where brackets denote the corresponding predictions from the CERN theoretical phase shifts. The single nucleon parameters are in fair agreement with the phase shift predictions.

The absorptive parameter $\text{Im}B_0$ has been calculated at threshold by Hachenberg *et al.*^{11,12} and by Bertsch and Riska.¹³ The theoretical value falls about 20% short of the empirical value. The parameter $\text{Im}C_0$ was calculated, using detailed balance, by Ericson and Ericson³ from $N + N \rightarrow NN\pi, d\pi$ reaction data, again in moderate agreement with the pionic atom value. No detailed comparison between theoretical and empirical values of $\text{Im}C_0$ can be made until the question of the Ericson-Ericson correction to this term is settled. The

real dispersive parts of B_0 and C_0 are discussed by Hüfner⁹ in his review article. He quotes theoretical estimates for the real parts to be opposite in sign and about 70% of the magnitude of the imaginary parts. For B_0 this agrees with a recent calculation of Mizutani and Koltun,¹⁴ and in sign with the calculation of Rockmore *et al.*¹⁵ The empirical estimates for $\text{Re}B_0$ and $\text{Re}C_0$ from pionic atoms are given in Ref. 9 as opposite in sign but equal in magnitude to the imaginary parts with an error of about 10%, and this is the value we have adopted.

In fact $\text{Re}B_0$ and $\text{Re}C_0$ are not determined independently of $\text{Re}\bar{b}_0$ and $\text{Re}c_0$ by experiment. A term in $B_0\rho^2$ can be expected to behave as $B_0\rho_{\text{avg}}\rho(r)$ with $\rho_{\text{avg}} \approx 0.17 \text{ fm}^{-3}$ for nuclear matter and less for a light nucleus. The effective parameters searched on are something like $\text{Re}(\bar{b}_0 + f_1 B_0)$ and $\text{Re}(c_0 + f_2 C_0)$ where f_1 and f_2 are both about 0.1. Taking the absorptive parameters given in the table above, $\text{Re}(B_0)$ increases the s -wave repulsion by about 40%, and $\text{Re}(C_0)$ decreases the p -wave attraction by about 10%. Actually, the p -wave is reduced by a somewhat larger amount as c_0 occurs inside the Ericson-Ericson term, which diminishes its effect, and C_0 does not. Pionic atom s -state level shifts are relatively insensitive to the absorption parameters (the imaginary parts of B_0 and C_0) and so determine $\text{Re}(\bar{b}_0 + f_1 B_0)$ relatively unambiguously. The s -state widths then determine $\text{Im}(B_0)$ with \bar{b}_0 and $\text{Re}(B_0)$ already determined. The parameters for pionic atom p states are strongly correlated. However, the single nucleon parameters are fairly near the phase shift values, while the absorptive parameter $\text{Im}(C_0)$ is determined only with large errors. Note that whereas there is some empirical information on the isospin dependence of the single nucleon parameters, there is no such information on the absorptive parameters.

In summary, the real part of the optical potential derived from pionic atom analysis differs from that calculated in lowest order scattering theory in that the repulsive part due to the s -wave pion-nucleon interaction is much stronger, and the attractive velocity dependent part due to the p -wave pion-nucleon interaction is weaker. The increase in s -wave repulsion is a marked effect, and, in the parametrization used, is attributed to the combined effect of the second order multiple-scattering term and the dispersive part of the s -wave absorption. The important point is that this increase is an empirical fact, regardless of the interpretation. The decrease in the attractive velocity dependent part is less firmly established, but is not inconsistent with a weakening due to the Ericson-Ericson effect and perhaps the dispersive part of the p -wave absorption term.

The optical potential we use to calculate the

scattering differs from that generally used for pionic atoms, the most important difference being the inclusion of the kinematic terms in $\nabla^2\rho$ and $\nabla^2\rho^2$. The term $C_0\nabla^2\rho^2$ has a negligible effect, but the term in $c_0\nabla^2\rho$ leads to an additional term in the s -wave part of the optical potential, arising from the pion-nucleon p -wave scattering, which makes an appreciable contribution to the scattering. Therefore, some adjustment must be made in the parameters. To make this adjustment, we calculate the s - and p -wave complex scattering lengths at 1 keV with the Coulomb potential omitted. We then vary the optical potential parameters by small amounts until approximate agreement is reached with the corresponding scattering lengths from the potential of Krell and Ericson,¹⁰ taken as a fit to the pionic atom data. The s -wave scattering length is defined as $a_0 = \delta_0/k$, and the p -wave scattering volume as $a_1 = \delta_1/k^3$. For this calculation, we take the real parts of B_0 and C_0 to be the same in magnitude but opposite in sign to the corresponding imaginary parts as mentioned above. Then $\text{Im}(B_0)$, $\text{Im}(C_0)$, \bar{b}_0 , and c_0 are varied. This fitting procedure is not unique, since one could also obtain a fit to the scattering lengths by, for example, fixing \bar{b}_0 , b_1 , c_0 , and c_1 at their phase shift values and varying the real and imaginary parts of B_0 and C_0 . We obtain two different sets of parameters, denoted 1 and 2, since Krell and Ericson¹⁰ quote two values of $\text{Im}(C_0)$ in their fits to pionic atom data; the higher value fits the p -state widths for heavier elements (KE 1), whereas the lower (KE 2) gives a better fit for light elements. The scattering lengths calculated from these two parameter sets are listed in Table II along with the values obtained from the Krell and Ericson potentials, and the experimental s -wave scattering lengths as tabulated in Hüfner.⁹ The latter are not completely model independent, but serve as an overall check on the s -wave parameters. The agreement between experimental and calculated s -wave lengths is reasonably good, with the exception of ⁴He.

One more modification to the pionic atom optical potential parameters must be made. The single nucleon parameters used in pionic atom analysis are purely real, as there is no possibility of quasi-elastic scattering. To account for quasielastic processes in pion-nucleus scattering, the imaginary parts of the single nucleon parameters must be included. These are given in the impulse approximation by the pion nucleon phase shifts. However, some correction must be made for the fact that the scattering occurs in nuclear matter. We have done this roughly, by multiplying the phase shift values by the Pauli factor obtained from the Goldberger¹⁶ classical calculation as given for

TABLE II. Zero-energy pion-nucleus s -wave scattering lengths a_0 (fm) and p -wave scattering volumes a_1 (fm³). The columns labeled KE 1 and KE 2 refer to values obtained from the optical potential given in Ref. 10. The columns labeled Set 1 and Set 2 are the corresponding values using the optical potential Eq. (5) with appropriate parameters.

	Exp.	KE 1	Set 1	KE 2	Set 2
⁴ He Rea_0	-0.133	-0.161	-0.163	-0.159	-0.151
Ima_0	0.042	0.069	0.080	0.069	0.083
Rea_1		0.734	0.687	0.780	0.728
Ima_1		0.294	0.222	0.205	0.153
¹² C Rea_0	-0.448	-0.442	-0.449	-0.438	-0.442
Ima_0	0.132	0.128	0.129	0.122	0.122
Rea_1		1.88	1.93	1.90	1.93
Ima_1		0.553	0.527	0.350	0.347
¹⁶ O Rea_0	-0.542	-0.570	-0.581	-0.570	-0.577
Ima_0	0.153	0.150	0.148	0.141	0.141
Rea_1		2.34	2.49	2.37	2.46
Ima_1		0.693	0.672	0.448	0.452

pions by Landau and McMillan.¹⁷ We use $k_F = 1.4$ fm⁻¹.

The optical potential parameters of sets 1 and 2 together with the Pauli factors are listed in Table III. We do not claim that they are the "best" parameters, only that they are representative. Note that we have used $\lambda = 1$, i.e., the full Ericson-Ericson effect. The best theoretical value, as determined by Thies,⁵ is $\lambda = 1.2$.

VI. GENERAL FEATURES OF THE ELASTIC CROSS SECTION

Low energy elastic scattering from light nuclei is principally sensitive to the interferences between Coulomb scattering, nuclear scattering from the repulsive s -wave part, and nuclear scattering from the attractive velocity dependent p -wave part of the optical potential. For $N = Z$ nuclei the elastic scattering is thus most sensitive to $(Re\bar{b}_0, ReB_0)$, (Rec_0, ReC_0) , and λ , the parameters in parentheses being strongly correlated. On the other hand, the total pion real absorption cross section is sensitive to ImB_0 and ImC_0 modified by the effect of the rest of the potential, just as level widths were in pionic atoms. Similarly, the total reaction cross section is sensitive to the complete imaginary part of the potential. (The behavior of these partial cross sections will be discussed in more detail in Sec. VIII.)

Some idea of the general behavior of the elastic cross section as a function of the parameters of the optical model is given by the Born approximation. As mentioned earlier, short range correlations suppress the effect of second order scatterings; so the Born approximation should provide a good estimate of the scattering from the velocity dependent part of the potential for light nuclei, provided the real absorptive effects on the incom-

ing wave are not too great. This is not true for scattering from the s -wave part of the potential.

If one ignores kinematical corrections and the absorptive terms, the scattering amplitude in Born approximation takes a very simple schematic form. Ignoring form factors and an overall normalization factor,

$$f_{\pm} \sim \pm \frac{1}{\sin^2\theta/2} + 4y^2 \sin^2\theta/2 - 2y^2(1-x), \quad (6)$$

TABLE III. Parameters for optical potential for low energy (30-50 MeV) pion-nucleus scattering.

	Real	Imaginary		
	Set 1			
b_0	-0.040 fm (-0.028 μ^{-1})	...		
b_1	-0.11 fm (-0.08 μ^{-1})	...		
B_0	-0.17 fm ⁴ (-0.04 μ^{-4})	0.17 fm ⁴ (0.04 μ^{-4})	...	
c_0	0.75 fm ³ (0.27 μ^{-3})	...		
c_1	0.62 fm ³ (0.22 μ^{-3})	...		
C_0	-0.79 fm ⁶ (-0.10 μ^{-6})	0.79 fm ⁶ (0.10 μ^{-6})	...	
$\lambda = 1$				
	Set 2			
b_0	-0.038 fm (-0.027 μ^{-1})	...		
b_1	-0.11 fm (-0.08 μ^{-1})	...		
B_0	-0.18 fm ⁴ (-0.05 μ^{-4})	0.18 fm ⁴ (0.05 μ^{-4})	...	
c_0	0.68 fm ³ (0.24 μ^{-3})	...		
c_1	0.62 fm ³ (0.22 μ^{-3})	...		
C_0	-0.41 fm ⁶ (-0.05 μ^{-6})	0.41 fm ⁶ (0.05 μ^{-6})	...	
$\lambda = 1$				
...	30 MeV	40 MeV	50 MeV	
Imb_0 (fm)	0.003	0.004	0.006	
Imb_1 (fm)	-0.001	-0.001	-0.002	
Imc_0 (fm ³)	0.007	0.015	0.029	
Imc_1 (fm ³)	0.004	0.007	0.014	
Pauli factor	0.19	0.24	0.31	

where y^2 is a parameter which measures the strength of the p -wave part of the potential relative to Coulomb, and the parameter x measures the strength of the s -wave repulsion relative to the p -wave attraction. The plus or minus signs correspond to π^+ or π^- scattering. The nuclear form factors have been ignored, but they have little influence on the general features of the cross section because they decrease slowly over the range of q^2 for scattering from a light nucleus at low energies. The parameters of Table III give y^2 to be about 24 for 50 MeV pions scattered from ^{12}C . Lowest order multiple-scattering theory gives a value of about $\frac{1}{12}$ for x at 50 MeV. Pionic atom parameters, with the effect of the dispersive parts of the absorption parameters ($\text{Re}B_0$ and $\text{Re}C_0$) included in the s -wave and p -wave strengths, give a value of about $\frac{1}{3}$ for x .

The schematic amplitude (6) for positive pion scattering has a minimum at $\sin^2\theta/2 = 1/2y$. Thus its position depends only on Coulomb interference with the nuclear scattering from the p -wave part of the nuclear potential. With $y^2 = 24$, the minimum occurs at 37° . The zeros of the amplitude are given by

$$\sin^2(\frac{1}{2}\theta) = \frac{1}{4}\{(1-x) \pm [(1-x)^2 - 4/y^2]^{1/2}\}.$$

For $y < 2$ there are no zeros. For $y > 2$ the number of zeros depends on the relationship of x to $x_0 = 1 - 2/y$ which is about 0.6 for 50 MeV pion scattering from ^{12}C . For $x < x_0$, there are two zeros lying on either side of the minimum in the amplitude. This results in a cross section with two minima separated by a maximum. As x increases, the zeros approach each other, and there is a single zero at the minimum when $x = x_0$. For $x > x_0$, there are no zeros, and thus the cross section is smooth with a single minimum. Numerically, the schematic amplitude gives minima at 17° and 88° with a maximum at 37° for the case with no s -wave repulsion ($x = 0$), and a single minimum at 37° for the case of very large s -wave repulsion ($x \geq x_0$).

The schematic amplitude for π^- has no turning points, but has a single zero. For small x this occurs at an angle larger than that for the π^+ amplitude minimum. As x increases the zero moves toward smaller angles. Thus the π^- cross section has only a single dip, whose position depends on the size of the s -wave repulsion. Numerically we expect a minimum at 92° for no s -wave repulsion,

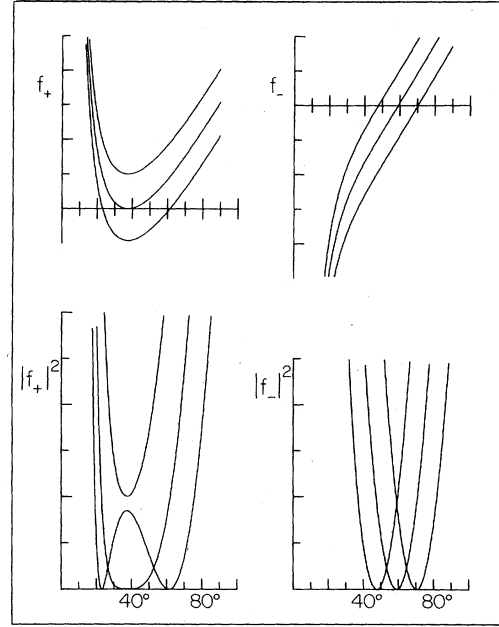


FIG. 1. Schematic amplitudes and corresponding cross sections for π^+ and π^- elastic scattering. The amplitudes are calculated from Eq. (6) with $y^2 = 24$ and $x = 0.4, 0.6,$ and 0.8 . The vertical scales are arbitrary. Top left are π^+ amplitudes, with the lowest of the three curves corresponding to $x = 0.4$. Top right are the π^- amplitudes, with the curve to the right corresponding to $x = 0.4$. At the bottom are the corresponding cross sections.

moving forward as the repulsion increases.

In Fig. 1 we plot the amplitudes (6) for $y^2 = 24$ and three values (0.4, 0.6, 0.8) of x . Top left are the amplitudes for π^+ . For $x = 0.4$ there are zeros at 60° and 24° with a minimum at 37° . For $x = 0.6$, i.e., $x = x_0$, the two zeros have moved together to the minimum and for $x = 0.8$ there is a single minimum at 37° . The corresponding cross sections are shown in the bottom left-hand side. Top right are the amplitudes for π^- . For $x = 0.4$ the zero in the amplitude is at 70° ; for $x = 0.8$ it has moved to 48° . The corresponding cross sections are shown in the bottom right-hand side of Fig. 1.

More realistically the Born approximation to the scattering amplitude for the kinematically correct version of the optical potential (3) is given, for an $N = Z$ nucleus and after removal of the Ericson-Ericson factor $L(r)$, by

$$F_B = \left[p_1 \bar{b}_0 + \frac{1}{p_1} c_0 \vec{k} \cdot \vec{k} - \frac{p_1 - 1}{2p_1} c_0 q^2 \right] A F(q^2) + \left[p_2 B_0 + \frac{1}{p_2} C_0 \vec{k} \cdot \vec{k} - \frac{p_2 - 1}{2p_2} C_0 q^2 \right] A^2 G(q^2) - \frac{1}{1 + \epsilon/A} \frac{2\omega \epsilon_\pi \alpha}{q^2} F_c(q^2), \quad (7)$$

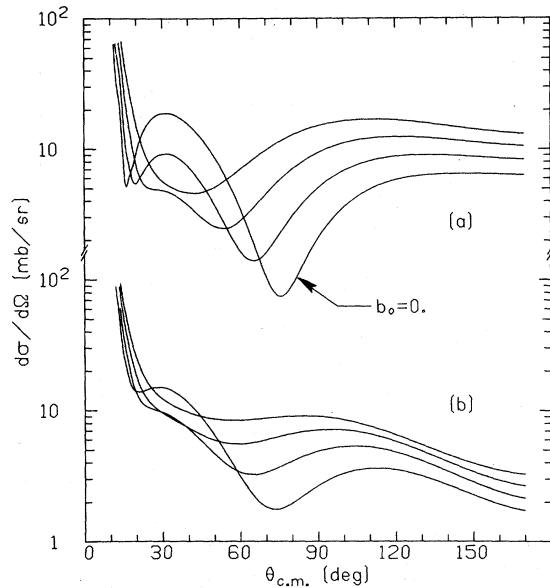


FIG. 2. Elastic scattering calculations for 50 MeV π^+ on ^{12}C . (a) Born approximation results for $\bar{b}_0 = 0, -0.04, -0.08, -0.12$. (b) Results from a full optical model calculation with the same values for \bar{b}_0 . Other parameters are from set 1.

where $F(q^2)$ and $F_c(q^2)$ are the Fourier transforms of the matter and charge densities respectively, normalized to $F(0) = 1$, while $G(q^2)$ is the corresponding Fourier transform of $\rho^2(r)$.

The results of several calculations for the elastic scattering of 50 MeV π^+ from ^{12}C in Born approximation are shown in the top half of Fig. 2.

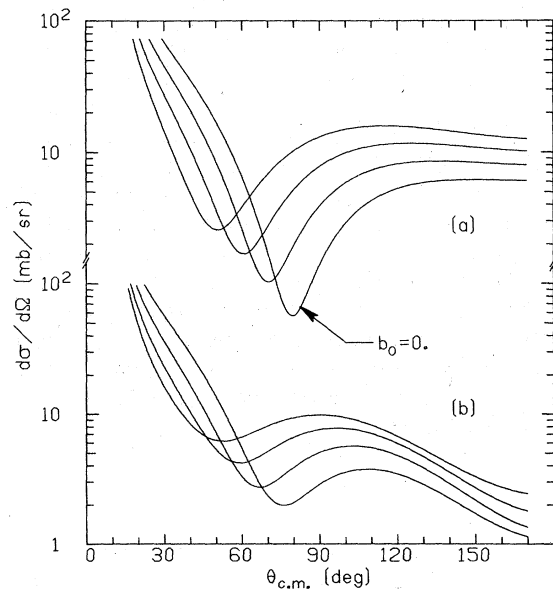


FIG. 3. Same as Fig. 2, except calculated for π^- elastic scattering.

The value of \bar{b}_0 , the single nucleon s -wave parameter, was varied from 0 to -0.12 fm in steps of -0.04 fm. The other parameters were taken from set 1. The qualitative features of the cross section are those suggested by the schematic amplitude (6). When there is little s -wave repulsion ($\bar{b}_0 = 0$) the minima are at 15° and 80° with a maximum at 35° , and these minima approach each other and coalesce into a single broad minimum at 35° as the repulsion is increased. The Born approximation for 50 MeV π^- elastic scattering from ^{12}C is shown in the top part of Fig. 3 for the same values of \bar{b}_0 . Note that the minimum is at 80° for $\bar{b}_0 = 0$ and that it moves forward toward 40° as the repulsion increases.

A similar set of calculations was done for 50 MeV π^+ on ^{12}C using the full optical model as explained in Sec. VII. These are shown in the lower halves of Figs. 2 and 3, and were done with the same values of \bar{b}_0 as were used in the Born approximation calculations. It is seen that the features of the Born approximation calculation remain. Thus we have shown that the shape of the scattering cross section for 50 MeV pions from light elements is particularly sensitive to the ratio of s -wave repulsion to p -wave attraction.

Figure 4 illustrates the interdependence of \bar{b}_0 and $\text{Re}B_0$. The dashed curves are calculated with the full optical potential (5) with $\text{Re}B_0 = 0$ and $\bar{b}_0 = 0, -0.04$ fm, and -0.08 fm respectively, the

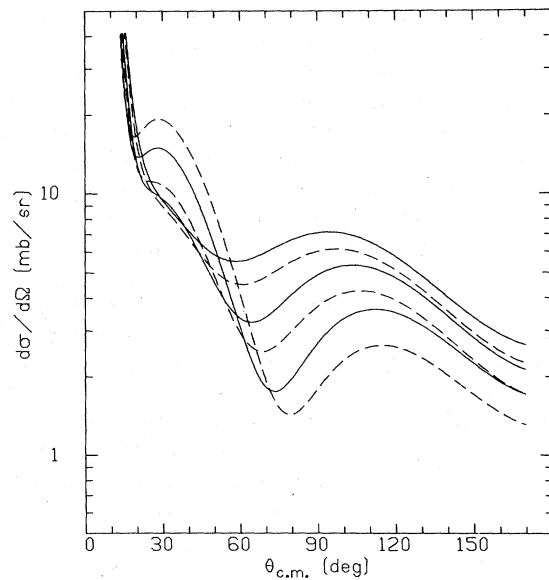


FIG. 4. Interdependence of $\text{Re}B_0$ and \bar{b}_0 in elastic scattering. The solid curves are optical model calculations for $\pi^+ - ^{12}\text{C}$ scattering with $\text{Re}B_0 = -0.17$ fm 4 and $\bar{b}_0 = 0, -0.04, \text{ and } -0.08$. The dashed curves are calculated with the same values for \bar{b}_0 but with $\text{Re}B_0 = 0$. Other parameters are from set 1.

other parameters being the parameters of set 1. The solid curves have $\text{Re}B_0 = -0.17 \text{ fm}^4$ as in set 1, and the same values of \bar{b}_0 as the dashed curves. It is seen that the effect of changing $\text{Re}B_0$ from 0 to -0.17 fm^4 is practically the same as changing \bar{b}_0 by -0.02 fm .

VII. ELASTIC SCATTERING CALCULATIONS

The elastic differential cross sections using the optical potential Eq. (5) are calculated by matching the wave function which solves Eq. (4) to the nonrelativistic Coulomb wave functions, giving the partial wave phase shifts. For this a modified version of the program PIRK¹⁸ was used. Parameter set 1 was used for all calculations, unless otherwise noted. The results of these calculations follow.

The results of the calculation for 50 MeV π^+ and π^- scattering from ^4He are compared to the experimental results of Crowe *et al.*¹⁹ in Fig. 5. As shown in Table I, the Krell and Ericson potential does not give the correct zero-energy s -wave scattering length for ^4He as deduced by Hüfner from pionic atom data. Consequently, the absorption parameters $\text{Re}B_0$ and $\text{Im}B_0$ were varied from the values in set 1 until a fit to this scattering length was obtained. The other parameters were left unaltered. The result of the scattering calculation using the new parameters is shown by

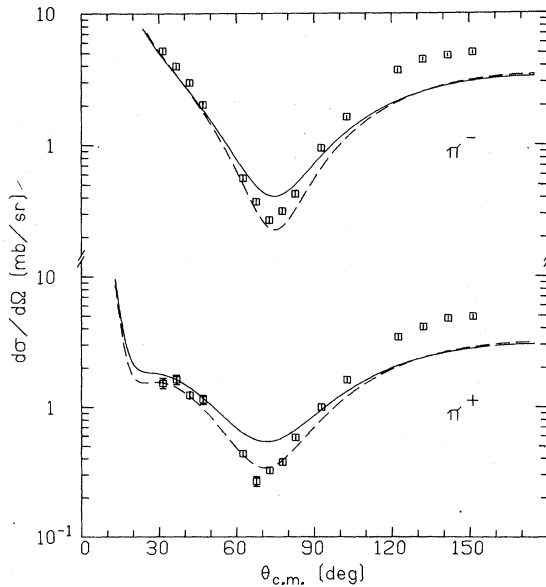


FIG. 5. Elastic scattering of 51 MeV π^+ and π^- on ^4He . The solid lines are calculated using the parameters of set 1. The dashed lines are calculations using parameters of set 1 with B_0 adjusted to fit the experimental s -wave scattering lengths: $\text{Re}B_0 = -0.06 \text{ fm}^4$, $\text{Im}B_0 = 0.05 \text{ fm}^4$. Data are from Ref. 19.

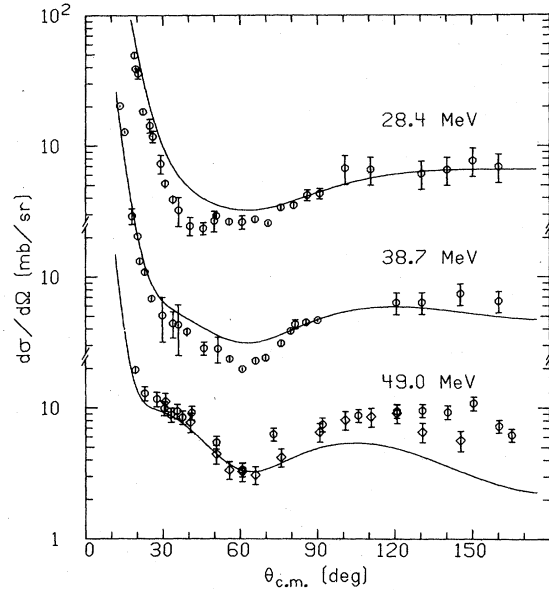


FIG. 6. Elastic scattering of π^+ on ^{12}C at 28.4, 38.7, and 49.0 MeV. The solid curves are the calculations using parameters of set 1. The circles are the data of Ref. 20; the diamonds are the data of Ref. 21.

the dashed line. It is in appreciably better agreement with the data.

We show calculations of the scattering of 28.4, 38.7, and 49.0 MeV π^+ from ^{12}C in Fig. 6 compared to the experimental data from the TRIUMF²⁰ group and Dytman *et al.*²¹ The calculations agree quite well with the data, at least as far as the general pattern is concerned. For instance, the change in interference pattern at forward angles is moderately well reproduced, as is the position of the minimum. The fact that the 50 MeV data show more interference pattern than the 30 MeV data is in accord with the schematic model. The velocity dependent p -wave attraction increases in going from 30 to 50 MeV, and the interference increases. Another important effect is that the absorptive part of the optical potential heavily damps any interference structure at 30 MeV.

Figure 7 shows a comparison of the calculated cross sections for 28.4 MeV π^+ and π^- mesons elastically scattered from ^{12}C , together with preliminary data from the TRIUMF group.^{20,22} The difference between π^+ and π^- scattering is mostly attributable to interference between Coulomb scattering and nuclear scattering as described by the schematic model.

Calculations for 40 and 50 MeV π^+ scattering from ^{16}O are compared with preliminary experimental results of Malbrough *et al.*²³ in Fig. 8. Also shown are the theoretical predictions for the scattering of 50 MeV π^- from this target.

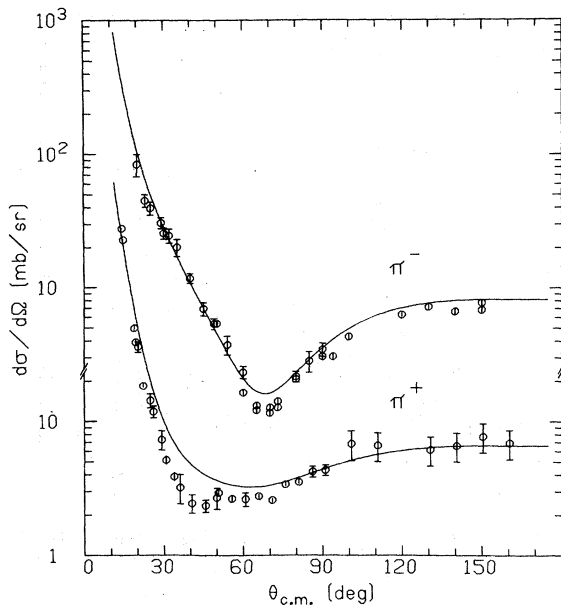


FIG. 7. Comparison of π^+ and π^- elastic scattering on ^{12}C at 28.4 MeV using parameter set 1. Data are from Refs. 20 and 22.

Figure 9 shows the theoretical predictions for the scattering of 50 MeV π^+ from ^{40}Ca , ^{90}Zr , and ^{208}Pb . A comparison of these calculations with the preliminary data of Malbrough *et al.* has been given by Freedman.²⁴ Again there is qualitative

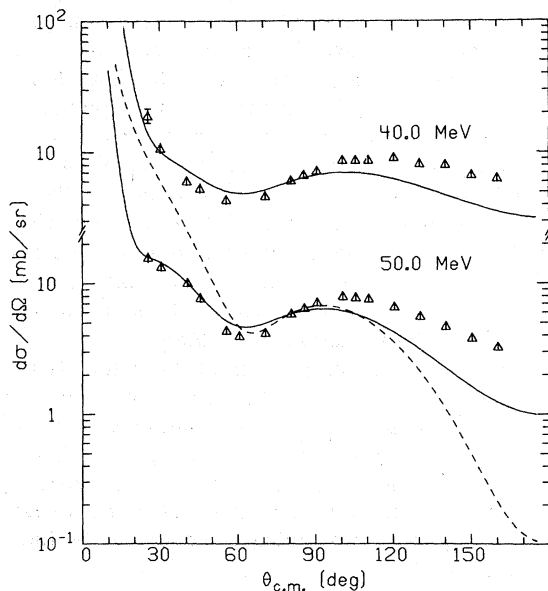


FIG. 8. Elastic scattering of pions from ^{16}O at 40 and 50 MeV. The data and solid lines are for π^+ scattering; the dashed line is the prediction for π^- scattering at 50 MeV. All calculations use parameters of set 1. Data are from Ref. 23.

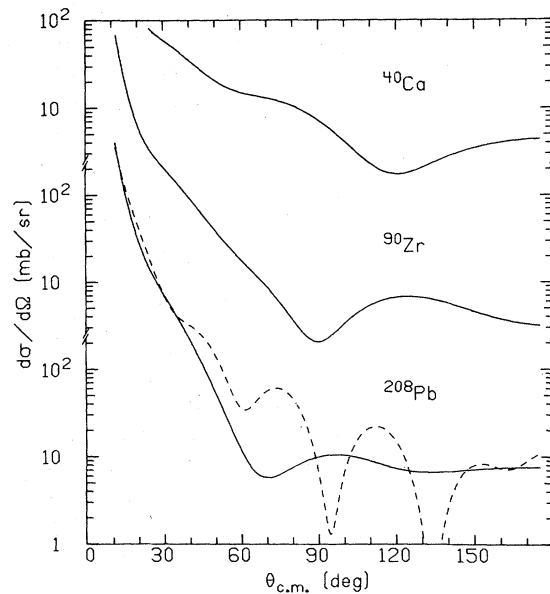


FIG. 9. Elastic scattering of pions on ^{40}Ca , ^{90}Zr , and ^{208}Pb at 50 MeV. The solid lines are for π^+ scattering, calculated with parameters from set 1. The dashed curve is the prediction for π^- scattering on ^{208}Pb .

agreement with experiments. Also shown is the prediction for the elastic scattering of 50 MeV π^- from ^{208}Pb . The π^- cross section, unlike the π^+ , shows a marked diffraction pattern. This illustrates another effect of the Coulomb potential: its interaction with a velocity dependent nuclear potential. The Coulomb field accelerates π^- mesons into the nuclear potential, so they feel a stronger p -wave potential than π^+ mesons which are slowed down by the nuclear charge distribution. For ^{208}Pb there is another effect in that π^- interacts more strongly with the neutron excess than π^+ , but this has a minor effect on the scattering cross sections. These Coulomb effects will be discussed further in the next section.

Overall the calculations give fair agreement with the data. The principal deficiency is in large angle scattering from light nuclei, where the calculations seem systematically low. The $\nabla^2\rho$ term in the optical potential arising from the angle transformation increases the backward angle scattering, but evidently not enough. An illustration of the sensitivity of the results to the absorption parameters is given in Fig. 10 for the scattering of 50 MeV π^+ from ^{12}C . The dashed curve (top) illustrates the effect of ignoring the Pauli principle in calculating the imaginary part of the optical potential due to quasielastic scattering, with a resultant increase by a factor of about 3 in this part of the optical potential. Comparing with Fig. 6 it is seen that using the absorptive parameters (set

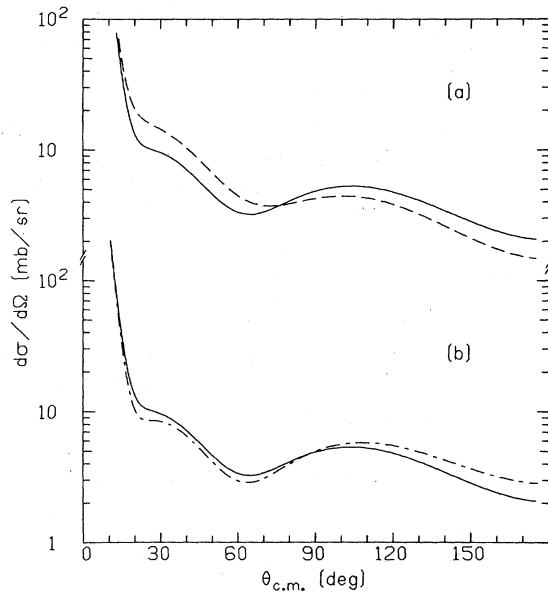


FIG. 10. Effects of parameter changes on elastic scattering cross sections. (a) Comparison of calculations with parameter set 1 (solid line) with those of set 2 (dashed line). (b) The solid line is the same as in (a); the dot-dashed line is a calculation using set 1 parameters but without the effect of the Pauli principle, i.e. the Pauli factor is set equal to one. The calculations were done for 50 MeV π^+ scattering on ^{12}C .

1) obtained from pionic atoms puts restrictions on the size of the contribution to the imaginary part of the optical potential from quasielastic scattering if any fit to the data is to be obtained. Also shown is the effect (dash-dot curve, bottom) of using parameter set 2, which used a reduced value of the p -wave absorptive potential. The difference between set 1 and set 2 is not great, so the uncertainty in the pionic atom absorption parameters does not greatly affect the calculation of elastic scattering.

As in the case of the real part of the optical potential, it is unlikely that from elastic scattering alone one can distinguish between the contributions of quasielastic scattering and absorption to the imaginary part of the optical potential. The two are strongly correlated and measurements of partial reaction cross sections are necessary to separate the two contributions.

We have taken the neutron distribution in ^{208}Pb to be the same as the proton distribution. To illustrate the sensitivity of the calculation to this assumption, we have made a calculation for a matter distribution, averaged over the neutron and proton distributions, with parameters $R = 6.69$, $\alpha = 0.542$, corresponding to the neutron distribution estimated by Boridy and Feshbach²⁵ in an early analysis of 1 GeV proton scattering. The

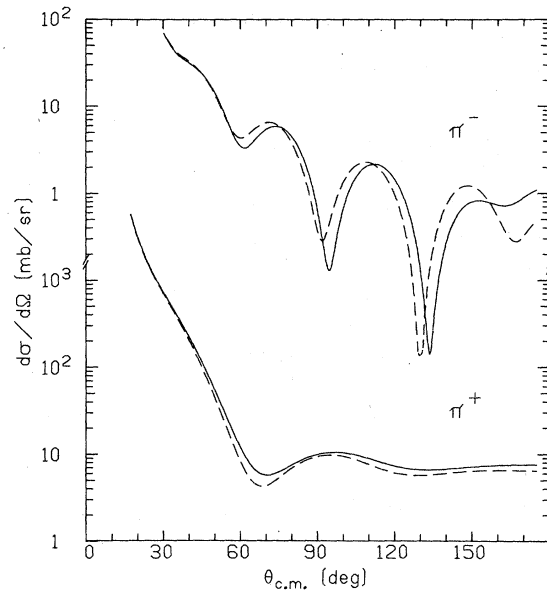


FIG. 11. Effect of varying the matter radius in 50 MeV pion elastic scattering on ^{208}Pb . The solid lines were calculated using $R_m = 6.46$ fm corresponding to the measured charge radius. The dashed line corresponds to $R_m = 6.69$ fm. Other parameters were from set 1.

result compared with the scattering obtained using the previous parameters is shown in Fig. 11. The difference for π^+ scattering is minor compared with that produced by variation of other parameters of the potential. The π^- diffraction scattering shows clearly the result of increasing the matter radius.

The effect of taking large excursions from what are effectively pionic atom parameters has been shown by Thies⁵ and by DiGiacomo *et al.*²⁶ to result in cross sections which differ markedly from experiment. Though the experiments are in a preliminary stage and could show considerable differences in detail when completed, their general features are not likely to change. Consequently we feel that the pionic atom parameters represent a good starting point for the analysis of low energy pion scattering.

We have used the multiple-scattering calculations of Ericson and Ericson,³ Thies,⁵ and Rostokin *et al.*⁶ to demonstrate why this should be so. As discussed in Sec. V, the result is independent of this mode of argument, which assumes a particular division between the contribution of single nucleon and absorptive parameters. It is only necessary for our argument that the parameters vary slowly with energy. Liu and Shakin²⁷ obtain similar results for the elastic scattering of 50 MeV π^+ from ^{12}C with a different balance between multiple scattering and absorption, as do Landau and Thomas.^{20,28}

VIII. REACTION CROSS SECTIONS

The total cross section σ_T is calculated from the optical theorem

$$\sigma_T = \frac{4\pi}{k} \text{Im} f_N(0^\circ), \quad (8)$$

where $f_N(0^\circ)$ is the elastic scattering amplitude in the forward direction from the non-Coulomb part of the optical potential.

The reaction cross section σ_R is given by

$$\sigma_R = -\frac{2\omega}{k} \int \phi^* (\text{Im} U_{\text{opt}}) \phi \, d\tau, \quad (9)$$

where ϕ are the distorted waves including Coulomb effects.

The reaction cross section can be split into two partial cross sections,

$$\sigma_R = \sigma_{qe} + \sigma_A,$$

where σ_A corresponds to the cross section for absorption of a pion and σ_{qe} is the cross section for all other reaction processes. These partial cross sections are more interesting than σ_R itself. As

$$\text{Im} U_{\text{opt}} = \text{Im} U_{\text{opt}}^{(a)} + \text{Im} U_{\text{opt}}^{(q)}, \quad (10)$$

where $U_{\text{opt}}^{(a)}$ has only terms involving the absorption parameters, we make an estimate of the absorption cross section from the ansatz

$$\sigma_A = -\frac{2\omega}{k} \int \phi^* (\text{Im} U_{\text{opt}}^{(a)}) \phi \, d\tau.$$

This clearly is not correct. Absorptive processes shadow the other inelastic processes, but the reverse is not true. A pion inelastically scattered can still be absorbed, a process which is

nearly independent of the target configuration. However, in the present case, with absorption parameters from pionic atoms and the imaginary part of the optical potential due to quasielastic scattering diminished by the Pauli effect, most of the attenuation in the elastic channel comes from the absorptive terms, so the ansatz may be a reasonable approximation.

The calculated total and partial cross sections are shown in Table IV. The table lists σ_A , σ_{qe} , σ_R , and σ_T for 50 MeV π^+ on ${}^4\text{He}$, ${}^{12}\text{C}$, ${}^{16}\text{O}$, ${}^{40}\text{Ca}$, ${}^{62}\text{Ni}$, ${}^{90}\text{Zr}$, and ${}^{208}\text{Pb}$ targets. In addition the predictions for 45 MeV π^- on ${}^{62}\text{Ni}$ and 60 MeV π^+ on ${}^{12}\text{C}$ are given, as there are existing measurements of σ_A for these projectile-target combinations. All calculations use parameter set 1 except for ${}^4\text{He}$, where the values of $\text{Re}B_0$ and $\text{Im}B_0$ which fit the zero-energy s -wave scattering lengths were used. The absorption cross section σ_A is in all cases much larger than the cross section for all other reaction processes σ_{qe} .

The reaction cross section σ_R for π^+ is only a fraction (about half) of the geometrical cross section $\pi(R+\lambda)^2$, showing that the interaction is in fact weak. The effect of the Coulomb potential together with a velocity dependent nuclear interaction is apparent in that the reaction cross section for π^- is larger than for π^+ . In ${}^{40}\text{Ca}$ the reaction cross section for π^- is 60% larger than for π^+ . For ${}^{208}\text{Pb}$, where Coulomb effects should be most pronounced, the diffraction pattern for π^- scattering is accompanied by a reaction cross section which is larger than the geometric cross section.

The particular cross sections listed in Table IV are estimated using parameters set 1, corresponding to the larger of the values for the p -wave ab-

TABLE IV. Partial cross sections (mb) for π^+ and π^- at 50 MeV on various targets. In addition values are given for 45 MeV π^- on ${}^{62}\text{Ni}$ and 60 MeV π^+ on ${}^{12}\text{C}$. Values of the geometrical cross section (GCS), taken as $\pi(R+\lambda)^2$, are included for comparison with σ_R .

Target	Proj.	T_π (MeV)	σ_{qe}	σ_A	σ_R	σ_T	GCS
${}^4\text{He}$	π^+	50	14	54	68	86	340
	π^-	50	15	59	74	95	
${}^{12}\text{C}$	π^+	50	34	126	160	228	510
	π^-	50	41	159	200	290	
${}^{16}\text{O}$	π^+	60	61	194	255	372	
	π^-	50	45	156	201	287	580
${}^{40}\text{Ca}$	π^+	50	57	209	266	390	
	π^-	50	90	314	404	591	800
${}^{62}\text{Ni}$	π^+	50	135	533	668	1069	
	π^-	45	159	826	985	1641	
${}^{90}\text{Zr}$	π^+	50	120	437	557	811	910
	π^-	50	198	818	1016	1718	
${}^{208}\text{Pb}$	π^+	50	136	538	674	975	1070
	π^-	50	252	1153	1405	2408	
${}^{208}\text{Pb}$	π^+	50	198	769	967	1365	1570
	π^-	50	508	2390	2898	5220	

TABLE V. Partial wave S matrix. Here $\eta = |S|$.

	^{16}O 40 MeV π^+			^{16}O 50 MeV π^+		
	ReS	ImS	η	ReS	ImS	η
$l=0$	0.735	-0.403	0.838	0.669	-0.354	0.757
1	0.787	0.268	0.831	0.708	0.285	0.763
2	0.945	0.160	0.958	0.882	0.243	0.915
3	0.996	0.028	0.996	0.989	0.056	0.991
4	1.000	0.003	1.000	0.999	0.008	0.999
5				1.000	0.001	1.000
	^{208}Pb 50 MeV π^+			^{208}Pb 50 MeV π^-		
	ReS	ImS	η	ReS	ImS	η
$l=0$	0.115	-0.334	0.353	-0.152	0.532	0.553
1	0.437	-0.180	0.473	0.135	0.105	0.171
2	0.538	0.142	0.556	-0.154	-0.103	0.185
3	0.624	0.288	0.687	0.204	-0.065	0.215
4	0.854	0.212	0.880	0.145	0.195	0.243
5	0.974	0.071	0.977	0.232	0.291	0.372
6	0.997	0.015	0.997	0.740	0.287	0.794
7	1.000	0.002	1.000	0.974	0.075	0.977
8				0.998	0.012	0.998
9				1.000	0.001	1.000

sorption parameters, $\text{Im}C_0$, given by Ericson. As indicated by Eq. (10) the absorption cross section depends on the absorption parameters $\text{Im}B_0$ and $\text{Im}C_0$. Thus if the parameters of set 2 are used, with $\text{Im}C_0 = 0.41 \text{ fm}^5$ as compared with $\text{Im}C_0 = 0.79 \text{ fm}^6$ for set 1, the absorptive cross section for π^+ on ^{12}C at 50 MeV drops from 126 to 98 mb. Measurements of σ_A and σ_{qe} are vital to an understanding of the reaction mechanisms of pions with nuclei.

Two estimates of σ_A have been reported in this energy range. Cassagnon²⁹ *et al.* give estimates of σ_R for 45 MeV π^- on ^{58}Ni , ^{60}Ni , and ^{62}Ni as 880, 1014, and 800 mb respectively. From the similarity of the emitted particle spectra to that from stopped pions, where only the absorptive process can occur, they infer that the bulk of the reaction cross section is due to absorption. For 45 MeV π^- on ^{62}Ni the calculations of Table IV give $\sigma_A = 826 \text{ mb}$ and $\sigma_{qe} = 159 \text{ mb}$, in qualitative agreement with the experimental observations. The absorption cross section for 60 MeV π^+ on ^{12}C has been measured by Byfield³⁰ *et al.* as $153 \pm 22 \text{ mb}$. The calculated values from Table IV are $\sigma_A = 194 \text{ mb}$ and $\sigma_{qe} = 61 \text{ mb}$. Pionic atom parameters thus seem to be of the right order of magnitude to give agreement with the present measurements of absorptive cross sections. A more precise measurement, however, would be desirable. It would also be interesting to measure the quasielastic cross sections directly. Strong back scattering of pions should be observed.

The elements of the partial wave S matrix are given in Table V for ^{16}O and ^{208}Pb . For 50 MeV π^+

on ^{16}O only the first three partial waves are important. For 50 MeV π^+ on ^{208}Pb partial waves up to $l=5$ contribute. Note the large inelasticities for 50 MeV π^- scattering from ^{208}Pb for partial waves up to $l=7$.

IX. INELASTIC SCATTERING CALCULATIONS

We have also performed some calculations for the excitation of low lying states by the inelastic scattering of pions. These were performed using the distorted wave impulse approximation code DWPI,²⁰ where the distorted waves were generated in the same way as in PIRK. The excitations were all calculated in the collective model. The theoretical predictions for the excitation by 50 MeV π^+ of the lowest 2^+ states in ^{12}C and ^{28}Si and the lowest 3^- states in ^{12}C and ^{208}Pb are shown in Fig. 12. The optical model parameters of set 1 were used, and the predictions for the ^{12}C states are compared with the experimental results of Dytman *et al.*²¹ The deformation parameters β used for these calculations were obtained from 35 MeV $p-p'$ data. These values of β are 0.60 for the 2^+ state in ^{12}C , 0.44 for the 3^- state in ^{12}C , 0.57 for the 2^+ state in ^{28}Si , and 0.126 for the 3^- state in ^{208}Pb . In Fig. 12 the results obtained by using the derivative of the standard optical potential of parameter set 1 for the form factor (solid line) are compared with the results using a form factor in which the imaginary part of the optical potential due to quasielastic scattering has been increased by ignoring the effect of the Pauli principle (dashed line). Figure 13 shows a similar comparison. Here the dashed

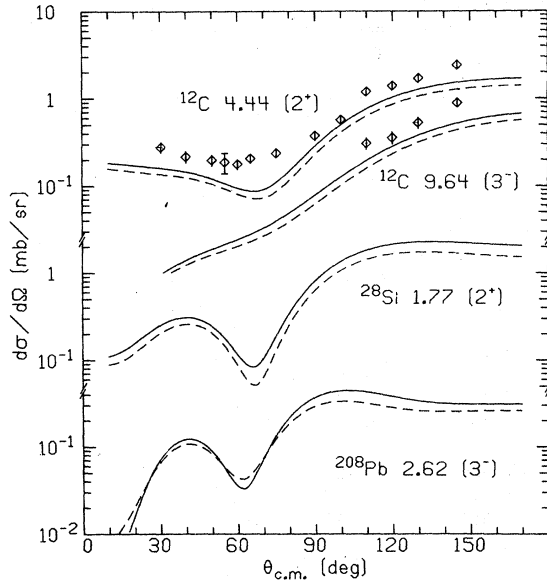


FIG. 12. Inelastic scattering of 50 MeV π^+ to states in ^{12}C , ^{28}Si , and ^{208}Pb using the collective model. The solid curves were calculated with the optical parameters of set 1 and the deformation parameters given in the text. The dashed curves show the effect of ignoring the Pauli principle. The data are from Ref. 21.

line is the result obtained by dropping from the inelastic form factor all the terms dependent on the absorption parameters B_0 and C_0 . The differences here are large. It is clear that the pion absorption-reemission process, in which the inter-

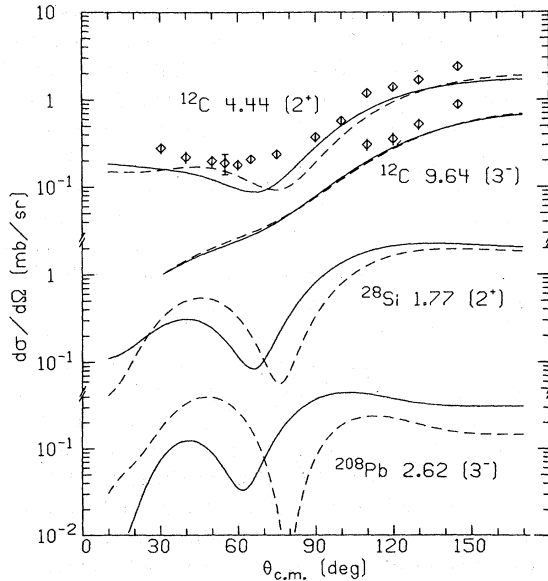


FIG. 13. Same as Fig. 12, except now the dashed curves show the effect of removing the absorptive terms when computing the inelastic form factor.

mediate state consists of two excited nucleons, can lead to inelastic scattering. In the present case most of the effect comes from $\text{Re}C_0$ which has the effect of diminishing the p -wave part of the inelastic form factor. Thus in this case there is destructive interference between inelastic scattering arising from multiple scattering and from the absorption-reemission processes. Whether this process is well represented by the deformation of the absorptive part of the optical potential is still to be determined.

The total cross section calculated for excitation of the 2^+ state of ^{12}C is 7.3 mb, for the 3^- state, 2.2 mb. Thus the reaction cross section for exciting these two states alone is 9.5 mb as compared with 34 mb from Table IV for the total nonabsorptive reaction cross section σ_{qe} .

X. EXTRAPOLATION TO HIGHER ENERGIES

It is of some interest to explore the extrapolation of the pion optical potential parameters to higher energies. The optical potential U_{opt} is built from the two basic interactions of the pion with the nucleus, the single nucleon part

$$V = \sum t_i, \quad (11)$$

where the t_i are the pion-nucleon scattering matrices, and the absorptive interaction V_A , which is a two-body operator in the nuclear coordinates,

$$V_A = t_i G t_A, \quad (12)$$

where t_A is the operator for absorption or emission of a pion on a single nucleon. In reality this operator will be more complicated, as other mesons can play a role in intermediate states, as discussed fully in Ref. 13. Also V_A and V are not independent unless carefully defined to be so.¹⁴

Ignoring these complications the optical potential U_{opt} , in the approximation that the number of pions in intermediate states is restricted to be 0 or 1, can be written as a power series in the operator W :

$$W = V + V_A G V_A$$

with

$$G = \frac{1}{E - H_0 + i\epsilon} = \frac{\mathcal{P}}{E - H_0} - i\pi\delta(E - H_0).$$

Then

$$U_{\text{opt}} = PW + PWQGW + \dots,$$

where Q is a projection operator projecting onto quasielastic channels, P is a projection operator onto the elastic channel, and \mathcal{P} stands for principal value.

The interpretation of the optical potential for low

TABLE VI. Extrapolated values of optical potential parameters.

	116 MeV	180 MeV	220 MeV
\bar{b}_0 (fm)	$-0.09 + i0.018$	$-0.12 + i0.032$	$-0.13 + i0.042$
b_1 (fm)	$-0.12 + i0.001$	$-0.12 + i0.008$	$-0.12 + i0.012$
B_0 (fm ⁴)	$0.0 + i0.22$	$0.0 + i0.26$	$0.0 + i0.26$
c_0 (fm ³)	$0.81 + i0.31$	$0.12 + i0.70$	$-0.23 + i0.52$
c_1 (fm ³)	$0.44 + i0.16$	$0.08 + i0.35$	$-0.11 + i0.26$
C_0 (fm ⁶)	$0.0 + i1.35$	$0.0 + i1.29$	$0.0 + i0.65$
Pauli factor	0.61	0.75	0.83
$\lambda=1$			

energy pion scattering has been that it is sufficient to write

$$U_{opt} = PV + PVQ \frac{\mathcal{P}}{E - H_0} V - i\pi PVQ \delta(E - H_0) V \\ + PV_A \frac{\mathcal{P}}{E - H_0} V_A - i\pi PV_A \delta(E - H_0) V_A, \quad (13)$$

where the terms involving the single nucleon operator V give rise to terms in the optical potential dependent on the single nucleon parameters. The term $PV_A[\mathcal{P}/(E - H_0)]V_A$ gives rise to the dispersive contribution of pion absorption to the optical potential and the term $-i\pi PV_A\delta(E - H_0)V_A$ gives rise to the imaginary part of the optical potential involving $\text{Im}B_0$ and $\text{Im}C_0$. In the low energy region this appears empirically to be the important contribution. The effects of multiple scattering and absorption appear independently. It is not clear that this approximation is sufficient at higher energies where the matrix elements become large. Nevertheless we will simply take the optical potential from (3) and extrapolate the parameters, as this at least includes all physical processes to lowest order.

The single nucleon parameters are then calculated from the CERN theoretical phase shifts with the same approximation for calculating \bar{b}_0 and for the effect of the Pauli principle on the imaginary parts as at low energy. As the absorptive operator V_A involves pion scattering from a nucleon and then absorption, we take the absorptive contributions to be proportional to the appropriate single nucleon scattering parameters. The absorptive parts of the optical potential $\sim\pi V_A\delta(E - H_0)V_A$ are then proportional to the squares of single nucleon parameters. Thus $\text{Im}B_0$ is taken, with spin-isospin averaging,^{11,12} to be

$$\text{Im}B_0 = K_1 [(\text{Re}b_0)^2 + (\text{Re}b_0 + 2\text{Re}b_1)^2].$$

For $\text{Im}C_0$ we assume (3, 3) dominance and write

$$\text{Im}C_0 = K_2 |c_0|^2.$$

The parameters $\text{Re}b_0$, $\text{Re}b_1$, and c_0 are calculated from the CERN theoretical phase shifts² and the

constants of proportionality K_1 and K_2 are obtained by fitting at 40 MeV to the values of parameter set 1. It is difficult to make an estimate for $\text{Re}B_0$ and $\text{Re}C_0$, except at very low energies. With better knowledge of the imaginary parts it would be possible to make an estimate of them using dispersion relations as has been attempted by Liu and Shakin.³¹ For the present we set them equal to zero, for lack of other information. The p -wave part of the optical potential becomes dominant at higher energies, so we expect results to be sensitive mainly to c_0 , $\text{Im}C_0$, and to a lesser extent to $\text{Re}C_0$. The optical model parameters obtained this way are given in Table VI for 116, 180, and 220 MeV pions. The absorptive parameter $\text{Im}C_0$ appears to have an unexpected behavior, as it is larger at 116 MeV than at 180 MeV where it would be expected to peak. However, the effect of this parameter in the explicitly velocity depen-

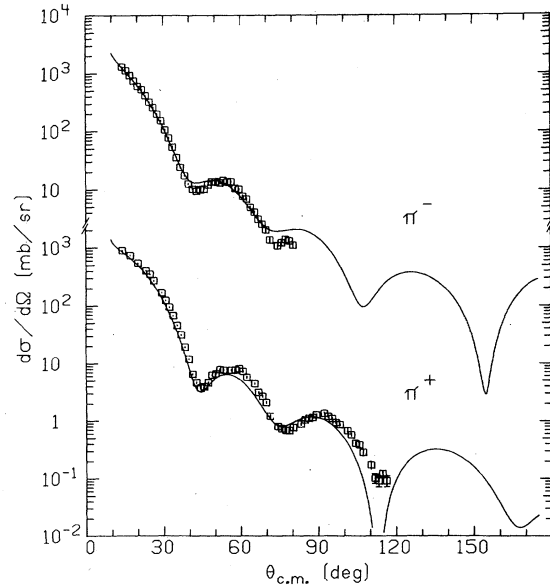


FIG. 14. Comparison of the elastic scattering of π^+ and π^- on ^{40}Ca at 116 MeV. The squares are preliminary data from SIN (Ref. 32). Calculations were done with the parameters of Table VI.

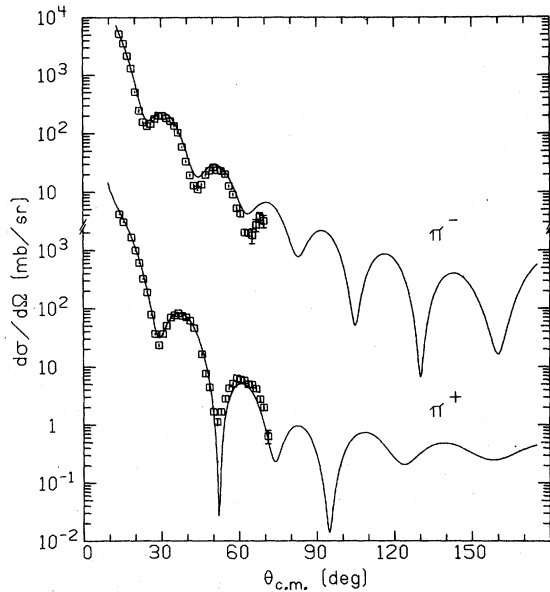


FIG. 15. Comparison of the elastic scattering of π^+ and π^- on ^{208}Pb at 116 MeV using the parameter of Tables I and VI. Data are from Ref. 32.

dent part of the potential is measured by $c_0 k^2$, and we have checked that $|c_0|^2 k^4$ reproduces approximately the pion-nucleon resonant total cross section.

Figures 14 and 15 show the calculated elastic scattering cross sections for π^+ and π^- at 116 MeV from ^{40}Ca and ^{208}Pb targets, compared with preliminary experimental data from SIN.³² The large difference between π^+ and π^- in the case of ^{208}Pb is seen to arise naturally from the interaction of the Coulomb field with the velocity dependent nuclear potential as discussed in Sec. VII. In Fig. 15 the neutron and proton distributions for ^{208}Pb were taken to have the same geometry. If the neutron geometry is varied, changes similar to those shown in Fig. 11 for 50 MeV negative pions are obtained. Figure 16 shows a comparison of 116 MeV π^+ and π^- inelastic scattering exciting the 3^- state in ^{208}Pb , using the collective model described in Sec. IX with the same value of $\beta = 0.126$. Again the phase difference between π^+ and π^- scattering arises directly from the effect of the Coulomb field. The dashed lines show the effect of eliminating absorption terms from the inelastic form factor. This has significant effects at large angles.

We have also made estimates of the partial cross sections for ^{12}C , ^{62}Ni , and ^{208}Pb for 30, 50, 180, and 220 MeV positive and negative pions. At 30 and 50 MeV we used the method of Sec. VIII, Eq. (10), which assumes that most of the attenuation of the incident beam comes from absorption. At higher energies this is not true, and it is neces-

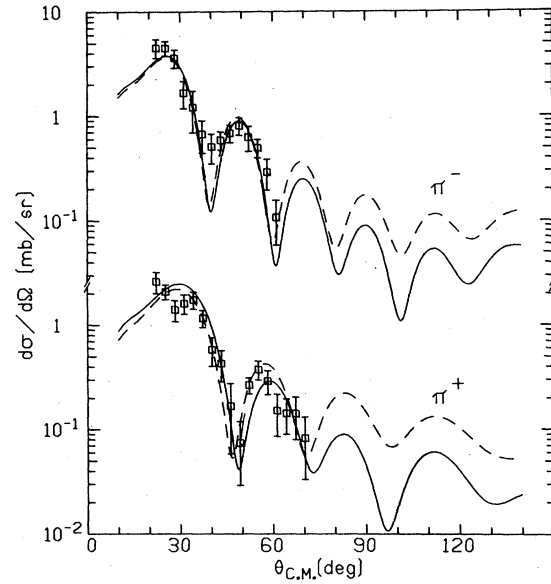


FIG. 16. Inelastic scattering of 116 MeV π^+ and π^- to the 2.62 MeV 3^- state of ^{208}Pb . The solid curves were computed with the collective model, and the parameters from Tables I and VI. The dashed curves show the effect of removing the absorptive terms when computing the inelastic form factor. Data are from Ref. 32.

sary to solve the coupled equations

$$\begin{aligned} T_A &= V_A + V_A G T, \\ T &= V + V G T + V_A G T_A, \end{aligned}$$

where T_A is the amplitude for absorption and T the scattering matrix for elastic and quasielastic scattering.

At sufficiently high energies, however, the Glauber approximation³³ should be adequate. In the optical limit, the relation for the reaction cross section σ_R becomes, with

$$\begin{aligned} \phi &\sim e^{ikz} \exp\left[-\frac{i}{v} \int_{-\infty}^z U_{\text{opt}}(\vec{b}, z') dz'\right], \\ \sigma_R &= \int d^2\vec{b} \left\{ 1 - \exp\left[\frac{2}{v} \int_{-\infty}^{+\infty} \text{Im} U_{\text{opt}}(\vec{b}, z) dz\right] \right\}, \end{aligned} \quad (14)$$

which becomes, in the limit of a local interaction of short range,

$$\sigma_R = \int d^2\vec{b} \left\{ 1 - \exp\left[-\sigma_{\text{tot}} \int_{-\infty}^{+\infty} \rho(\vec{b}, z) dz\right] \right\}, \quad (15)$$

where σ_{tot} is the total pion-nucleon cross section.

When real absorption on a single nucleon is possible, Glauber³² has shown that in this limit

$$\sigma_A = \int d^2\vec{b} \left\{ 1 - \exp\left[-\sigma_{\text{abs}} \int_{-\infty}^{+\infty} \rho(\vec{b}, z) dz\right] \right\}, \quad (16)$$

where σ_{abs} is the cross section for absorption on a

single nucleon, and

$$\sigma_{qe} = \sigma_R - \sigma_A. \quad (17)$$

Relation (16) has an obvious generalization

$$\sigma_A = \int d^2\vec{b} \left\{ 1 - \exp \left[\frac{2}{v} \int_{-\infty}^{+\infty} \text{Im} U_{\text{opt}}^{(a)}(\vec{b}, z) dz \right] \right\}, \quad (18)$$

where $\text{Im} U_{\text{opt}}^{(a)}$ is the imaginary part of the optical potential due to absorption. Translating this into distorted wave language, we have

$$\sigma_A = \frac{-2\omega}{k} \int \phi_a^* (\text{Im} U_{\text{opt}}^{(a)}) \phi_a d\tau, \quad (19)$$

where ϕ_a are distorted waves distorted by that part of the optical potential due to absorption only.

The physical meaning of (19) is that absorption is shadowed only by the absorption process itself, i.e., that pions scattered elastically or inelastically are absorbed at the same rate as unscattered pions. For the pion case, with a strongly velocity dependent interaction, this is only likely to be true near resonance where the variation of the optical potential with energy is at a minimum. At low energies an inelastically scattered pion sees a weaker interaction than one elastically scattered. Consequently we have calculated the partial cross

TABLE VII. Energy dependence of estimated partial cross sections (mb). The method of estimation is explained in the text.

Element	T (MeV)	σ_{qe}	σ_A	σ_R	σ_T
π^+					
^{12}C	30	11	103	114	158
	50	34	126	160	228
	180	224	160	384	581
^{62}Ni	220	247	71	318	521
	30	38	306	344	467
	50	120	437	557	811
^{208}Pb	180	485	551	1036	1730
	220	618	291	909	1645
	30	53	436	489	584
^{208}Pb	50	197	769	966	1365
	180	623	1216	1839	3270
	220	915	755	1670	3196
π^-					
^{12}C	30	14	138	152	232
	50	41	159	200	290
	180	230	170	400	615
^{62}Ni	220	255	75	330	552
	30	73	789	862	1445
	50	198	818	1016	1718
^{208}Pb	180	534	647	1181	2018
	220	703	323	1026	1898
	30	199	2742	2941	5342
^{208}Pb	50	508	2390	2898	5220
	180	749	1639	2388	4365
	220	1196	918	2114	4140

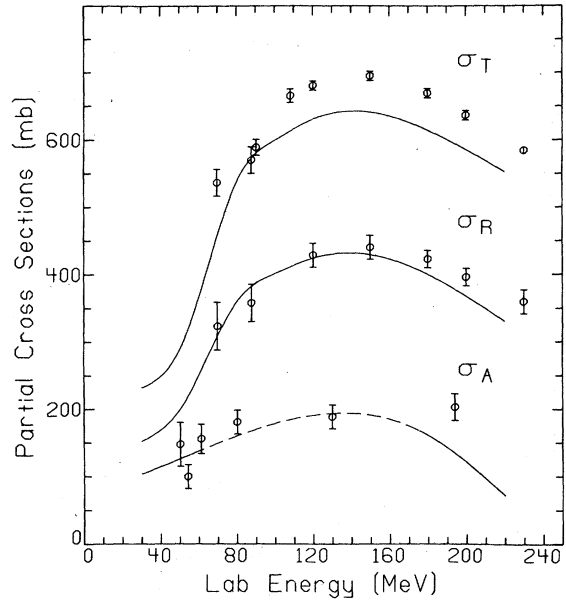


FIG. 17. Partial cross sections as a function of energy for ^{12}C . The total and reaction cross sections (σ_T and σ_R) are for negative pions. The absorption cross sections (σ_A) are for positive pions. The calculations are described in the text. Data for σ_T and σ_R are from Ref. 36; data for σ_A are from Ref. 37.

sections using (17) and (19) for pion energies of 180 and 220 MeV and used the method of Sec. VIII, i.e., Eq. (10) at 30 and 50 MeV. The results are shown in Table VII.

The quasielastic scattering cross section rises steadily with energy. The absorption cross section varies much less in this energy range. At very low energies, of course, it must obey a $1/v$ law and fall off past the resonance unless new processes come in. Bellotti *et al.*³⁴ have measured the absorption cross section for 130 MeV π^+ on ^{12}C in a bubble chamber. They obtain the value $\sigma_A = 189 \pm 19$ mb. Interpolation between the numbers in Table VII gives a comparable estimate (see Fig. 17). Jackson *et al.*³⁵ give cross sections for the emission of nucleons with energy greater than 60 MeV from a ^{62}Ni target, averaged over π^+ and π^- , as being $\sigma = 550 \pm 200$ mb for 100 MeV pions and 750 ± 200 mb for 220 MeV pions. If these are interpreted as measurements of σ_A , then the predicted cross section is too low for energies above the resonance.

Figure 17 shows a comparison of the theoretical total and reaction cross sections for π^- mesons on ^{12}C with the experimental results tabulated by Binon *et al.*³⁶ Also shown in Fig. 17 are the theoretical predictions for the absorption cross sections for π^+ mesons on ^{12}C , compared with the experimental results collected by Ginocchio.³⁷ Note that the dashed part of the theoretical curve is not

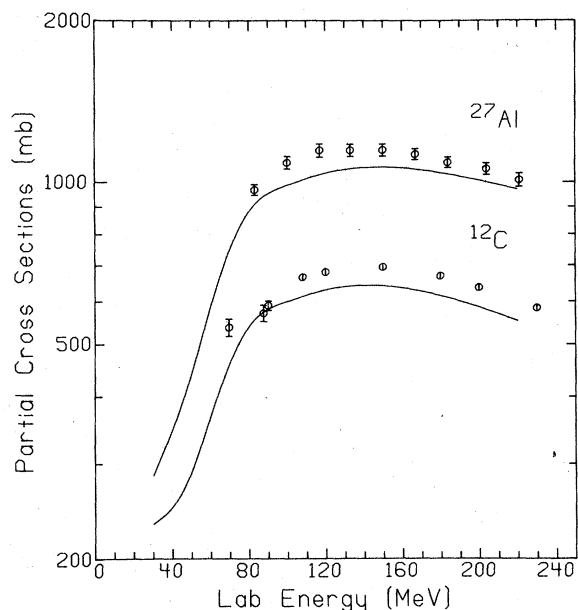


FIG. 18. Comparison of the total cross sections for ^{12}C and ^{27}Al as a function of energy. Data for ^{12}C are from Ref. 35; for ^{27}Al from Ref. 38.

calculated but interpolated from the calculated values at 30, 50, 180, and 220 MeV. The reaction cross section is given quite well by the theoretical calculation, but the theoretical total cross section is about 10% low in the resonance region. The predicted σ_A agrees well at low energies but falls below experiment in the resonance region. Figure 18 shows a comparison of calculated and measured total cross sections for π^- mesons on ^{12}C and π^+ mesons on ^{27}Al . The experimental points for ^{12}C are the same as in Fig. 17. The experimental points for ^{27}Al are taken from the work of Carroll *et al.*³⁸ In both cases the theoretical predictions are about 10% too low in the resonance region, and for ^{27}Al the calculation does not reproduce the shallow maximum in the experimental curve at about 110 MeV.

This illustrates a systematic defect of the calculated total cross sections. Total cross sections for π^- mesons on ^4He over a range of energies have been measured by Binon *et al.*³⁹ Carroll *et al.*³⁸ have measured total cross sections for π^+ mesons for many targets over a similar range of energies. The theoretical predictions do not reproduce the systematics of these measured total cross sections. The predicted maxima are too small and in the wrong position, being too low in energy for π^- on ^4He and too high in energy for π^+ on ^{208}Pb .

XI. SUMMARY

The main purpose of this paper was to extrapolate optical model parameters obtained from the

analysis of pionic atom data to the case of low energy pion-nucleus scattering. The shape of the low energy elastic scattering cross sections for light elements is particularly sensitive to the relative strength of the repulsive and velocity dependent attractive terms in the optical potential. This relative strength is fairly well established by pionic atom data, and is in fair agreement with low energy scattering data. The other principal feature of this extrapolation is that absorption is the dominant reaction channel at low energies. The calculated absorption cross sections are in reasonable agreement with what little experimental evidence there is. Pionic atom data and low energy elastic scattering data very likely determine only four real parameters. Measurement of total and partial reaction cross sections would give much more information, but a more complete theoretical treatment is necessary as well, if the roles of multiple scattering and absorption processes in reaction mechanisms are to be clearly delineated. This is particularly true of the dispersive contributions from absorption, which can be important in determining the real part of the optical potential and, via the collective model, in inelastic scattering to individual final states. It would be more satisfactory if the connection between pionic atoms and low energy scattering were more directly established by using the same form of the optical potential for the analysis of both types of experiment.

A simple extrapolation was made, via the pion-nucleon phase shifts, of optical model parameters from the pionic atom case to higher energy scattering. This had reasonable success in explaining the difference between π^+ and π^- elastic scattering at 116 MeV as being due to the interplay between the Coulomb field and the velocity dependent part of the optical potential. However, the systematic behavior of the total and partial reaction cross sections was not given correctly. This is not surprising considering the crudeness of the extrapolation, but illustrates again the point that elastic scattering by itself does not give too much information on interaction mechanisms. The various partial cross sections provide more stringent tests of any model and are necessary to get information on the important physical processes.

ACKNOWLEDGMENTS

We wish to thank R. A. Eisenstein for providing us with codes PIRK and DWPI.¹⁸ Thanks are also due to K. L. Erdman and R. R. Johnson of U. B. C., R. A. Eisenstein of C. M. U., and E. Boschitz of S. I. N. for furnishing tabulated preliminary experimental data. We especially thank M. Thies,

V. Rostokin, and D. O. Riska for many illuminating discussions. This research was supported in part by a grant from the National Science Foundation.

APPENDIX: ORIGIN OF KINEMATIC FACTORS IN THE OPTICAL POTENTIAL

We give here a brief derivation of the optical potential U_{opt} from the pion-nucleon transition matrix t . Since U_{opt} is needed in the pion-nucleus center of mass (ACM), whereas t is known in the pion-nucleon center of mass (2CM), various kinematic factors appear. The treatment follows that of Ref. 6.

We consider only first order terms and the semi-local Kisslinger factorizable approximation

$$U_{\text{opt}}^{\text{ACM}}(\vec{k}, \vec{k}') = \hat{t}^{\text{ACM}}(\vec{k}, \vec{k}')\rho(q), \quad (\text{A1})$$

where $\vec{q} = \vec{k}' - \vec{k}$, $\rho(q)$ is the Fourier transform of the single particle density normalized to $\rho(0) = A$, and \hat{t}^{ACM} denotes the pion-nucleon scattering amplitude t^{ACM} averaged over nucleon momenta. In what follows let (\vec{k}, ω) and (\vec{k}', ω') be the initial and final momenta and energies of the pion, (\vec{p}, E) and (\vec{p}', E') be those of the struck nucleon. Unsubscripted variables are assumed to be in the ACM system; the subscript c.m. refers to the 2CM system. Then

$$t^{\text{ACM}}(\vec{p}'\vec{p}\vec{k}'\vec{k}) = K t^{2\text{CM}}(\vec{k}_{\text{c.m.}}, \vec{k}'_{\text{c.m.}}), \quad (\text{A2})$$

where

$$K = \left[\frac{(EE'\omega\omega')_{2\text{CM}}}{(EE'\omega\omega')_{\text{ACM}}} \right]^{1/2} \simeq \frac{\omega_{\text{c.m.}}}{\omega} \quad (\text{A3})$$

$$\vec{k}_{\text{c.m.}} \cdot \vec{k}'_{\text{c.m.}} = \frac{1}{(1+\epsilon)^2} \left\{ \vec{k} \cdot \vec{k}' (1+\epsilon/A)^2 - \frac{1}{2} \epsilon (1-1/A) q^2 - \epsilon \vec{P} \cdot (\vec{k} + \vec{k}') (1+\epsilon/A) + \epsilon^2 P^2 - (\epsilon^2/4)(1-1/A)^2 q^2 \right\}. \quad (\text{A8})$$

We drop the last two terms as they are of order ϵ^2 . The term linear in P vanishes when Fermi-averaged as it gives a term proportional to the Fourier transform of the probability current density, which vanishes for a spin zero nucleus. Thus we have

$$2\bar{\omega} U_{\text{opt}}^{\text{ACM}}(\vec{k}, \vec{k}') = -4\pi \frac{1+\epsilon}{1+\epsilon/A} \left\{ b_0 + \frac{c_0}{(1+\epsilon)^2} \left[(1+\epsilon/A)^2 \vec{k} \cdot \vec{k}' - \frac{1}{2} \epsilon \frac{A-1}{A} (1+\epsilon/A) q^2 \right] \right\} \rho(q), \quad (\text{A9})$$

where $\bar{\omega}$ is the reduced energy of the pion in the ACM:

$$\bar{\omega} = \frac{\omega}{1+\epsilon/A}.$$

The absorptive parts of the optical potential are

and

$$t^{2\text{CM}} = -4\pi \frac{1}{2\bar{\omega}_{\text{c.m.}}} (b_0 + c_0 \vec{k}_{\text{c.m.}} \cdot \vec{k}'_{\text{c.m.}}). \quad (\text{A4})$$

Here $\bar{\omega}_{\text{c.m.}}$ is the reduced energy of the pion

$$\bar{\omega}_{\text{c.m.}} = \frac{\omega_{\text{c.m.}}}{1+\epsilon}, \quad \epsilon = \frac{\omega}{M}$$

and momentum conservation gives

$$\vec{p} + \vec{k} = \vec{p}' + \vec{k}'.$$

To first order in ϵ

$$\vec{k}_{\text{c.m.}} = \frac{\vec{k} - \epsilon \vec{p}}{1+\epsilon}, \quad \vec{k}'_{\text{c.m.}} = \frac{\vec{k}' - \epsilon \vec{p}'}{1+\epsilon}. \quad (\text{A5})$$

The nucleon momentum \vec{p} may be divided into two parts, one the momentum of the nucleon due to the center of mass motion of the nucleus as a whole, the other the Fermi motion of the nucleons relative to the nucleus center of mass. Thus

$$\vec{p} \simeq -\frac{1}{A} \vec{k} + \vec{p}_f, \quad \vec{p}' \simeq -\frac{1}{A} \vec{k}' + \vec{p}'_f. \quad (\text{A6})$$

We use momentum conservation and transform to new variables,

$$\vec{P} = \frac{1}{2}(\vec{p}_f + \vec{p}'_f)$$

and

$$(\vec{p}_f - \vec{p}'_f) = (1-1/A)\vec{q}. \quad (\text{A7})$$

Substitution of (A6) and (A7) into (A5) gives

treated in a similar manner. As they involve the center of mass system of two nucleons and a pion, the factors $(1+\epsilon)$ which occur in the single nucleon terms become $(1+\epsilon/2)$. The inclusion of these terms and the Ericson-Ericson effect leads to Eq. (5) in the text, after transformation to coordinate space.

- ¹L. S. Kisslinger, *Phys. Rev.* **98**, 761 (1955).
- ²Particle Data Group, Report No. UCRL-20030, 1970 (unpublished).
- ⁴J. M. Eisenberg, J. Hüfner, and E. J. Moniz, *Phys. Lett.* **47B**, 381 (1973).
- ⁵M. Thies, *Phys. Lett.* **63B**, 43 (1976).
- ⁶G. E. Brown, B. K. Jennings, and V. Rostokin (unpublished).
- ⁷At. Data Nucl. Data Tables **14**, 479 (1974).
- ⁸*Landolt-Börnstein: Nuclear Radii*, edited by H. R. Colard, L. R. B. Elton, and R. Hofstadter (Springer, Berlin, 1967), New Series, Group I, Vol. 2.
- ⁹Jörg Hüfner, *Phys. Rep.* **21C**, 1 (1975).
- ¹⁰M. Krell and T. E. O. Ericson, *Nucl. Phys.* **B11**, 521 (1969).
- ¹¹F. Hachenberg, J. Hüfner, and H. J. Pirner, *Phys. Lett.* **66B**, 425 (1977).
- ¹²F. Hachenberg and H. J. Pirner, *Ann. Phys. (N.Y.)* **112**, 401 (1978).
- ¹³G. Bertsch and D. O. Riska, *Phys. Rev. C* **18**, 317 (1978).
- ¹⁴T. Mizutani and D. S. Költun, *Ann. Phys.* **109**, 1 (1977).
- ¹⁵R. Rockmore, P. Goode, and H. McManus, *Phys. Rev. Lett.* **37**, 1720 (1976).
- ¹⁶M. L. Goldberger, *Phys. Rev.* **74**, 1270 (1948).
- ¹⁷Rubin H. Landau and Malcolm McMillan, *Phys. Rev. C* **8**, 2094 (1973).
- ¹⁸R. A. Eisenstein and G. A. Miller, *Comput. Phys. Commun.* **8**, 130 (1974); **11**, 95 (1976).
- ¹⁹K. M. Crowe, A. Fainberg, J. Miller, and A. Parsons, *Phys. Rev.* **180**, 1349 (1969).
- ²⁰H. Dollard, K. L. Erdman, R. R. Johnson, J. R. Johnson, T. Masterson, and P. Walden, *Phys. Lett.* **63B**, 416 (1976); R. R. Johnson, T. G. Masterson, K. L. Erdman, A. W. Thomas, and R. H. Landau, *Nucl. Phys.* **A296**, 444 (1978).
- ²¹S. A. Dytman, J. F. Amann, P. D. Barnes, J. N. Craig, K. G. R. Doss, R. A. Eisenstein, J. D. Sherman, W. R. Wharton, R. J. Peterson, G. R. Bureson, S. L. Verbeck, and H. A. Thiessen, *Phys. Rev. Lett.* **38**, 1059 (1977); **39**, 53 (1977); *Bull. Am. Phys. Soc.* **22**, 4 (1977).
- ²²R. R. Johnson *et al.* in Proceedings of the Zurich Conference on Intermediate Energy Physics, 1977 (unpublished); *Phys. Lett.* **78B**, 560 (1978).
- ²³D. J. Malbrough, R. D. Edge, C. W. Darden, T. Marks, B. M. Freedom, F. Bertrand, T. P. Cleary, E. E. Gross, C. A. Ludemann, R. L. Burman, R. P. Redwine, K. Gotow, and H. A. Moinester, *Bull. Am. Phys. Soc.* **22**, 4 (unpublished); Los Alamos Report No. LA-UR-77-1939 (unpublished); *Phys. Rev. C* **17**, 1395 (1978).
- ²⁴B. Freedom, in Proceedings of the Zurich Conference on Intermediate Energy Nuclear Physics, 1977 (unpublished).
- ²⁵E. Boridy and H. Feshbach, *Phys. Lett.* **50B**, 433 (1974).
- ²⁶N. J. DiGiacomo, A. S. Rosenthal, E. Rost, and D. A. Sparrow, *Phys. Lett.* **B66B**, 421 (1977).
- ²⁷L. C. Liu and C. M. Shakin, *Phys. Rev. C* **16**, 333 (1977).
- ²⁸R. H. Landau and A. W. Thomas, *Phys. Lett.* **61B**, 361 (1976).
- ²⁹V. Cassagnou *et al.*, *Phys. Rev. C* **16**, 741 (1977).
- ³⁰H. Byfield, J. Kessler, and L. M. Ledeman, *Phys. Rev.* **86**, 17 (1952).
- ³¹L. C. Liu and C. M. Shakin, *Phys. Rev. C* (to be published).
- ³²E. Boschitz, in Proceedings of the Zurich Conference on Intermediate Energy Nuclear Physics, 1977 (unpublished); Q. Ingram, E. Boschitz, L. Pflug, J. Zichy, J. P. Albanèse, and J. Arvieux, *Phys. Lett.* **76B**, 173 (1978).
- ³³R. J. Glauber, in *Lectures in Theoretical Physics*, edited by W. E. Brittin and L. G. Dunham (Interscience, N.Y., 1959), Vol. I, p. 315.
- ³⁴E. Bellotti, D. Cavalli, and C. Matteuzzi, *Nuovo Cimento*, **18A**, 75 (1973).
- ³⁵H. E. Jackson, S. B. Kaufman, L. Meyer-Schutzmeister, J. P. Schiffer, S. L. Tabor, S. E. Vigdor, J. N. Worthington, L. L. Rutledge, Jr., R. E. Segel, R. L. Burman, P. A. M. Gram, R. P. Redwine, and M. A. Yates, *Phys. Rev. C* **16**, 730 (1977).
- ³⁶F. Binon, P. Duteil, J. P. Garron, J. Gorres, L. Hugon, J. P. Peigneux, C. Schmit, M. Spighel, and J. P. Stroot, *Nucl. Phys.* **B17**, 168 (1970).
- ³⁷J. N. Ginocchio, *Phys. Rev. C* **17**, 195 (1978).
- ³⁸A. S. Carroll, J.-H. Chiang, C. B. Dover, T. P. Kycia, K. K. Li, P. O. Mazur, D. N. Michael, P. M. Mockett, D. C. Rahm, and H. Rubinstein, *Phys. Rev. C* **14**, 635 (1976).
- ³⁹F. Binon, P. Duteil, M. Gouanere, L. Hugon, J. Jansen, J.-P. Lagnaux, H. Palevsky, J.-P. Peigneux, M. Spighel, and J.-P. Stroot, *Phys. Rev. Lett.* **35**, 145 (1975).